

Improvement Of Power Quality By Hybrid Energy Conversion System Using High Gain Integrated Boost Converter

M.PALA PRASAD REDDY

Assistant Professor, Dept of EEE, AITS Rajampet

P.B.CHENNAIAH

Assistant Professor, Dept of EEE, AITS Rajampet

T.SWAPNA

(M.Tech), E.P.E Student, Dept of EEE, AITS Rajampet

ABSTRACT

This paper proposes PV/battery hybrid energy conversion system with the application of modified instantaneous symmetrical components theory to micro grid side bidirectional voltage source converter (μ G-VSC). This μ G-VSC is actively controlled to inject the generated active power into the grid along with harmonic and reactive power compensation for unbalanced and non linear load at point of common coupling (PCC), such that the current drawn from grid is purely sinusoidal at unity power factor (UPF). High gain integrated cascaded boost (HGICB) converter topology is used to track the maximum power point tracking (MPPT) with high gain and less current ripple. A model of a hybrid PV Energy Conversion System is developed & simulated in MATLAB/SIMULINK environment. The effectiveness of the proposed control strategies for HGICB converter and μ G-VSC with battery energy conversion system are validated through extensive simulation studies.

Index Terms— PV energy conversion system, high gain integrated cascaded boost dc-dc converter, instantaneous symmetrical components theory, battery energy storage system.

1. INTRODUCTION

Renewable energy is the energy which comes from natural resources such as sun light, wind, rain tide and geothermal heat [1]. Among these alternative sources the electrical energy from photovoltaic (PV) cells is currently regarded as a natural energy source that is more useful, since it is free abundant, clean and distributed over the earth [2]. The efficiency of energy conversion from PV cells is currently low and the initial cost for its implementation is high. Thus it is necessary to use novel techniques to extract the maximum power from the panels [3], such as incremental conductance [INC], constant voltage (CV) and perturbation and observation [p&o]. INC and p&o techniques are most commonly used to track the maximum power [4].

The output voltage of PV arrays is relatively low. In order to satisfy the high bus voltage requirements for full bridge, half bridge or multi level grid inverters, the PV series connected configurations are the conventional solution. The grid connected PV system employing the cascaded H-bridge multi level inverters or other multi level configurations is introduced to optimize the PV output power [5]. The converter topology is a high gain integrated cascaded boost converter having n -converters connected in cascade using a single active switch. The instability caused by the cascade structure is avoided, when compared with the conventional cascade boost converter. This class of converters can be used only when the required number of stages is not very large, else the efficiency will be reduced. Depending on their operation in ac micro grid, power converter can be classified into (i) grid feeding (ii) grid supporting and (iii) grid forming power converters [7][8]. For the control of μ G-VSC in micro grid many control algorithms are available, they are synchronous reference theory, power balance theory and direct current vector control [9][10]. Compared to above control strategies the instantaneous symmetrical component based control proposed in this paper for micro grid is applications simple in formulation, avoids interpretation of instantaneous reactive power and needs no complex transformations.

This paper is organized as follows: In section II, system description and modeling of various components are presented. The proposed control strategies for HGICB DC-DC Converter, Battery Converter and μ G-VSC are discussed in section III. The simulation results are presented in section IV. With concluding remarks in section V.

II. SYSTEM DESCRIPTION

The proposed system consists of PV/Battery hybrid system with the main grid connecting to non linear and unbalanced loads at the PCC as shown in the Fig. 1.

The photovoltaic system is modeled as non linear voltage sources [8]. The PV array is connected to HGICB dc-dc converter and bidirectional battery converters are shown in Fig. 1, which are coupled at the dc side of a μ G-VSC. The HGICB dc-dc converter is connected to the PV array works as MPPT controller and battery converter is used to regulate the power flow between dc and ac side of the system.

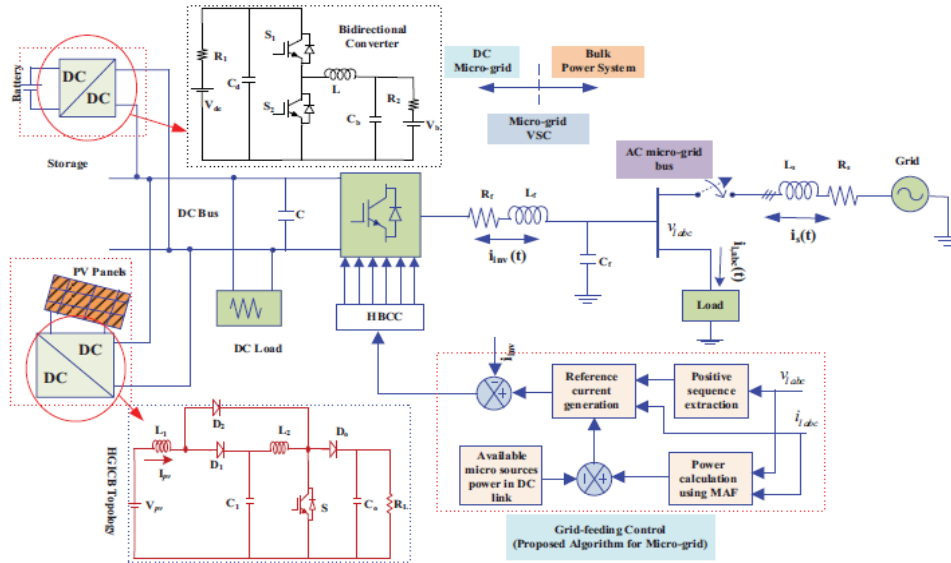


Fig.1 Hybrid Energy conversion system under consideration

III. MODELING AND CONTROL

The MPPT algorithm for HGICB Converter, control approaches for battery converter and μ G-VSC are discussed in the following sections.

PV Array Model

The PV cells are usually represented by a simplified equivalent circuit model as shown in fig.2

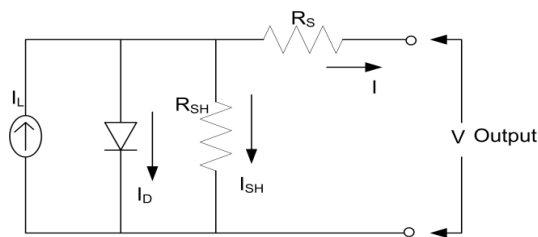


Fig.2 Equivalent Circuit of PV Cell

The PV cell output voltage, which is-temperature and solar irradiation level, can be expressed

$$I = I_{ph} - I_o \left\{ \exp \left(V + \frac{IRs}{nsVt} \right) - 1 \right\} - V + \frac{IRs}{Rsh} \tag{1}$$

The thermal voltage of the diode is related to the junction temperature as given by

$$Vt = \frac{KTA}{q} \tag{2}$$

Battery Converter Modeling

The single phase equivalent circuit of battery converter shown in fig.3. There are two dc sources including high side bus voltage V_H and low side battery source V_L representing both voltage sources of bidirectional dc-dc converter. The average inductor current i_L and output current i_o can flow in both directions. R_1 represents high side internal resistances in charging and discharging mode, R_2 represents low side internal resistance for both charging and discharging. C_H and C_L are bus capacitor bank and output capacitor. Two active switches Q_1 and Q_2 controlled by gating control of Gate1 and Gate2.

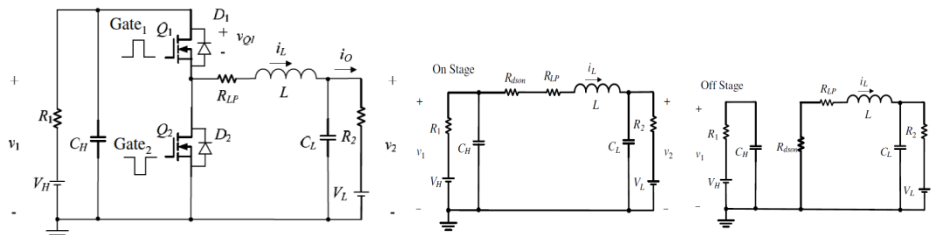


Fig.3 Equivalent circuit of battery converter

The battery converter goes through two topological stages in each switching period, its power stage dynamics can be described by a set of state equations. The average state space model of the converter can therefore be given as

$$\begin{aligned} \frac{di_L}{dt} &= \frac{V_{c1}d(t)}{L} - \frac{V_{c2}}{L} - \frac{(r_s + r_L)i_L}{L} \\ \frac{dV_{c1}}{dt} &= \frac{L}{V_{dc} \cdot Bus - V_{c1}} - \frac{i_L d(t)}{C_1} \\ \frac{dV_{c2}}{dt} &= \frac{C_1 R_1}{V_B - V_{c2}} - \frac{i_L}{C_2} \end{aligned} \tag{3}$$

The averaged model is nonlinear and time-invariant because of the duty cycle, $d(t)$. This model is finally linearized about the operating point to obtain a small-signal model as shown in Fig. 4.

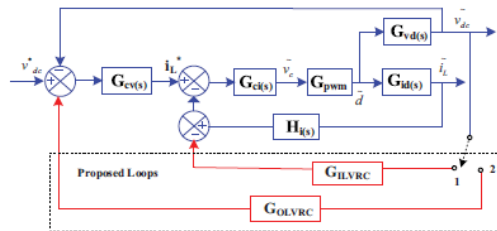


Fig.4 Inner and outer loops of battery converter with MACMC

The important transfer functions used to design the compensators and to analyze the system behavior under small signal conditions (i) the duty-cycle-to output transfer function $G_{cv}(s)$, carries the information needed to determine the type of the voltage feedback compensation, (ii) the duty-cycle-to-inductor current transfer function $G_{ci}(s)$, is needed to determine the current controller structure.

Proposed Controller for Battery Converter

If AC side of μ G-VSC has constant power appliances (CPAs), in the small-signal sense, CPAs nature leads to negative incremental input-conductance which causes destabilization of the dc-link voltage [13]. On the micro grid generation side, the inherent negative admittance dynamics of their controlled conversion stages challenges the dc-link voltage control and stability. This effect is more with reduced dc-link capacitance. Therefore, in both cases, fast and effective control and stabilization of the dc-link voltage is very crucial issue. To address this problem, many methods are reported in the literature i.e (i) by large DC link capacitance (ii) by adding passive resistances at various positions in DC LC filter (iii) by loop cancellation methods [12], [13]. In this paper, a new modified-ACMC (MACMC) control algorithm is proposed for effective control and stabilization of battery converter by introducing virtual resistance (VR) in (i) outer loop called outer loop virtual resistance control (OLVRC) (ii) intermediate loop called inner loop virtual resistance control (ILVRC) as shown in Fig. 5.

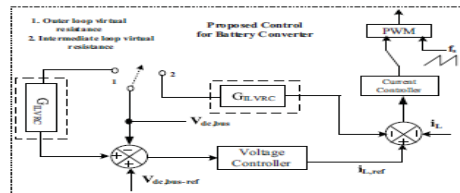


Fig.5 A new modified ACMC control strategy for battery converter

The proposed virtual resistance based dynamic damping methods aim at injecting a damping signal that compensate for negative conductance caused by CPAs without any power loss.

Design steps for Compensators of Battery Energy Storage System

The effectiveness of proposed VRCs control algorithm is investigated and compared with the use of traditional ACMC [14]. The flowchart for modes of operation of battery converter is shown in Fig. 6.

The design guidelines for inner and outer loop compensators of ACMC are given below. The inner loop (current) gain can be written as

$$T_i(s) = G_{id}(s) R_i G_{ci}(s) F_m \tag{4}$$

The outer loop (voltage) gain can be written as:

$$T_v(s) = G_{vd}(s) G_{cv}(s) (1 + G_{ci}(s)) F_m \tag{5}$$

and the overall loop gain therefore can be written as:

$$T_1(s) = T_s + T_v \tag{6}$$

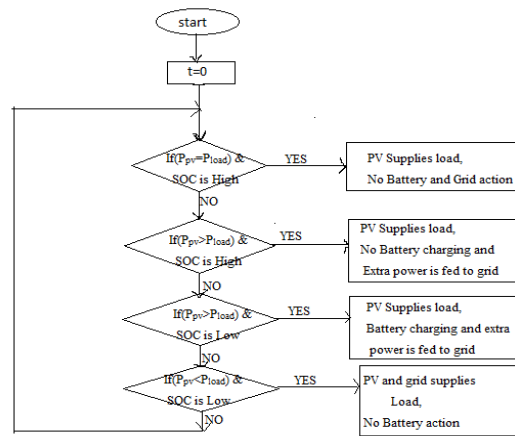


Fig.6 Flow chart of power flow in hybrid system.

Voltage Loop Design Steps:

- i) Place one zero as high as possible, yet not exceeding resonating frequency of the converter.
- ii) Place one pole at frequency of output capacitor ESR to cancel the effects of output capacitor ESR.
- iii) Adjust, gain of compensator to trade-off stability margins and closed-loop performance.
- iv) Another pole should be place at origin to boost the dc and low frequency gain of the voltage loop.

Similar steps mentioned above are followed to design current loop and for design of MACMC loops. Following the design procedure given above, the inner current and outer voltage loop compensators are designed to regulate the DC link voltage to 920 V. ***Generation of reference currents for μ G-VSC***

The main aim of the μ G-VSC control is to cancel the effects of unbalanced and harmonic components of the local load, while supplying pre-specified amount of real and reactive powers to the load. Upon successfully meeting this objective, the grid current i_g will then be balanced and so will be the PCC voltage v_p provided, grid voltage v_g is balanced. Let us denote the three phases by the subscripts a, b and c. Since i_g is balanced, we can write:

$$i_{ga} + i_{gb} + i_{gc} = 0 \quad (7)$$

From the Fig. 1, Kirchoff's current law (KCL) at PCC gives

$$i_{g, abc} + i_{inv, abc} = i_{L, abc} \quad (8)$$

Therefore, from (5) and (6), we can write as:

$$i_{inv, a} + i_{inv, b} + i_{inv, c} = i_{L, a} + i_{L, b} + i_{L, c} \quad (9)$$

Since i_g is balanced due to the action of the compensator, the voltage v_p will also become balanced. Hence, the instantaneous real powers P_g will be equal to its average component. Therefore, we can write

$$P_g = v_{pa}i_{ga} + v_{pb}i_{gb} + v_{pc}i_{gc} \quad (10)$$

solving above equations, the μ G-VSC reference currents are obtained as follows

$$\begin{aligned}
 i_{inv,a}^* &= i_{la} - \frac{vga + \beta(vgb - vgc)}{\Delta} (P_{lavg} - P_{\mu s} + P_{loss}) \\
 i_{inv,b}^* &= i_{lb} - \frac{vgb + \beta(vgc - vga)}{\Delta} (P_{lavg} - P_{\mu s} + P_{loss}) \\
 i_{inv,c}^* &= i_{lc} - \frac{vgc + \beta(vga - vgb)}{\Delta} (P_{lavg} - P_{\mu s} + P_{loss})
 \end{aligned}
 \tag{11}$$

Where,

$$\Delta = \sum_{j=a,b,c} V_{gj}^2, \quad \beta = \tan \varphi \square \quad \sqrt{3} = \frac{Q_s}{P_s \sqrt{3}}$$

And $Q_s = Q_l - Q_{\mu s}$, and by substituting $\beta P_s = \frac{Q_s}{\sqrt{3}}$ into the equation (9), the modified Grid side voltage source converter (G-VSC) reference current equations in terms of active and reactive components are obtained as:

$$\begin{aligned}
 i_{inv,a}^* &= i_{la} - \frac{vga P_s}{\sum_{j=a,b,c} v_{2gj}} - \frac{(vgb - vgc) Q_s}{\sum_{j=a,b,c} v_{2gj} \sqrt{3}} \\
 i_{inv,b}^* &= i_{lb} - \frac{vgb P_s}{\sum_{j=a,b,c} v_{2gj}} - \frac{(vgc - vga) Q_s}{\sum_{j=a,b,c} v_{2gj} \sqrt{3}} \\
 i_{inv,c}^* &= i_{lc} - \frac{vgc P_s}{\sum_{j=a,b,c} v_{2gj}} - \frac{(vga - vgb) Q_s}{\sum_{j=a,b,c} v_{2gj} \sqrt{3}}
 \end{aligned}
 \tag{12}$$

In equations (9) and (10), $P_{\mu s}$, P_{lavg} , and Q_l are the available micro source power, average load power, and load reactive power respectively. P_{loss} denotes the switching losses and ohmic losses in actual compensator. The term P_{lavg} is obtained using a moving average filter of one cycle window of time T in second.

IV. RESULTS AND DISCUSSION

The general simulation model for PV/Battery hybrid energy conversion system using HGICB is shown in fig.7.

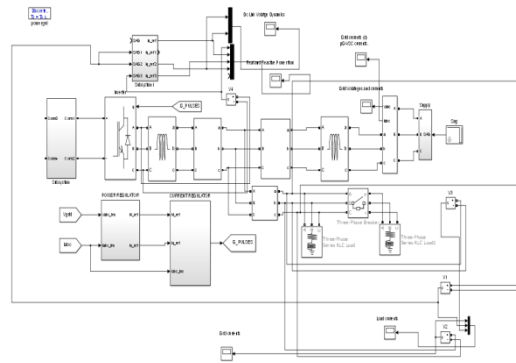
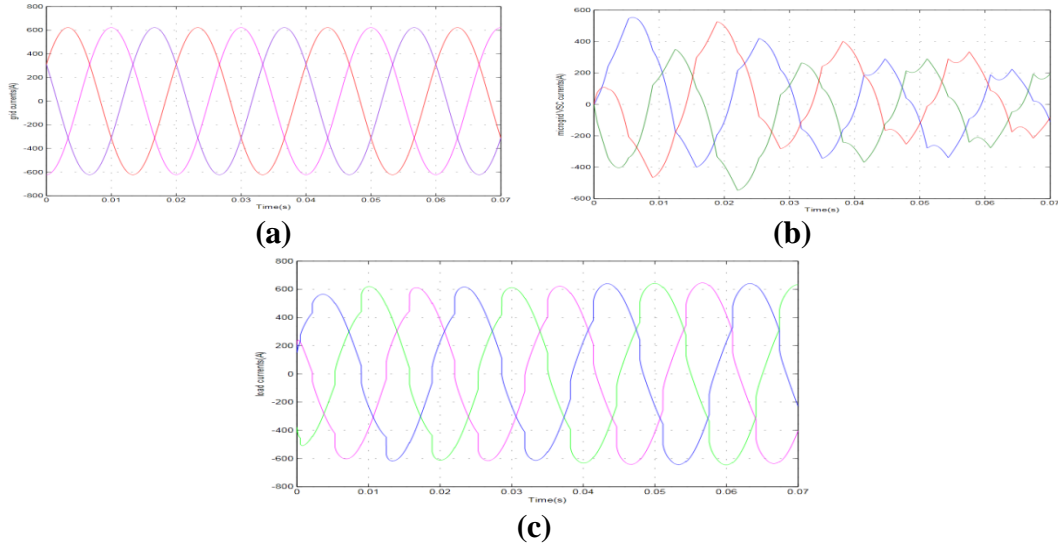


Fig.7 simulink model of hybrid energy conversion system

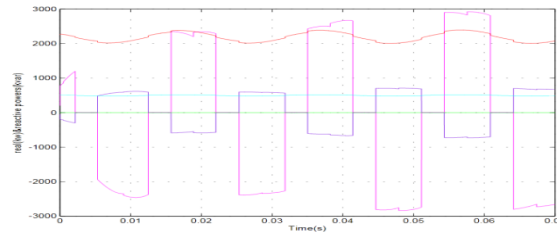
Performance of μ G-VSC with different solar radiation levels:

The μ G-VSC is actively controlled to inject the generated active power as well as to compensate the harmonic and reactive power demanded by the unbalanced and non-linear load at PCC, such that the current drawn from grid is purely sinusoidal at UPF. The dynamic compensation performance of μ G-VSC using proposed control algorithm with insolation change and non linear unbalanced load currents along with grid side currents are shown in Fig (8).



Fig(8):Simulation results using control approach for micro grid side VSC (a) micro grid VSC currents (b) grid currents (c) load currents

When insolation $G = 200 \text{ W/m}^2$, the maximum power extracted from PV arrays is 2.5kW and the total dc load power (4.5 kW) is partly supplied by PV arrays and the remaining dc load power (2kW) is drawn from grid through the bidirectional $\mu\text{G-VSC}$. Here observed that the power flows from ac side to dc link as shown in the Fig (9).



Fig(9): Real and Reactive power flow waveforms of PV hybrid generating system

When insolation $G = 1000 \text{ W/m}^2$, the maximum power available from PV arrays is 12.5kW, part of this power (4.5 kW) is supplied to dc load and remaining power (8 kW) is supplied to the ac load through bidirectional $\mu\text{G-VSC}$. In this case, the power flows from dc link to ac side. This shows the bidirectional power flow capability of $\mu\text{G-VSC}$. These dynamics of power flows is shown in Fig(10).The corresponding variations in the grid current against grid voltage with upf are shown in Fig.10 along with dc link voltage variations.

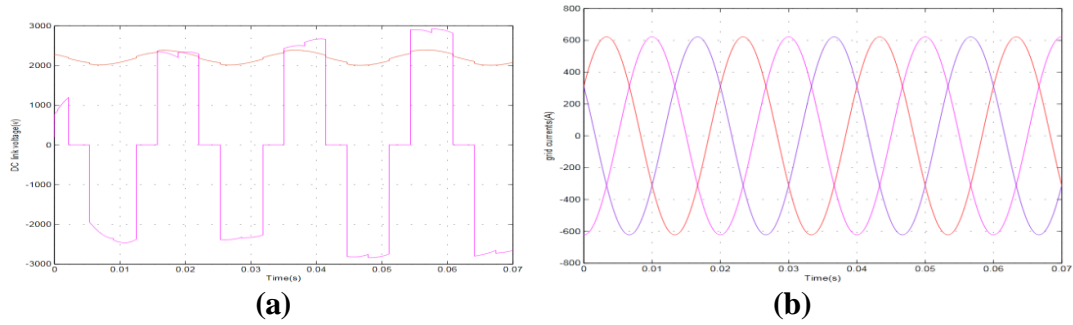


Fig.10 (a) dc link voltage dynamics with different insulations (b) Grid voltages and currents

EXTENSION WORK

The extension for the proposed system is multi-level interlude converter is connected to PV array. The simulation model for proposed hybrid system is shown in fig.11

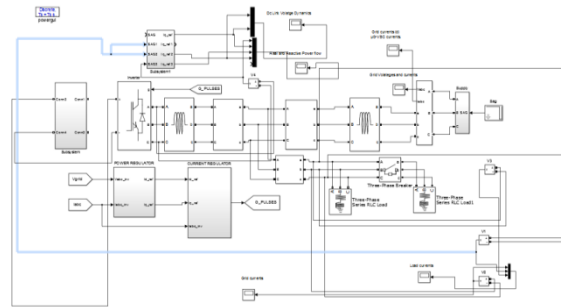


Fig.11 simulink model of hybrid system using multilevel converter

The simulation results using multi level converter is shown in figs

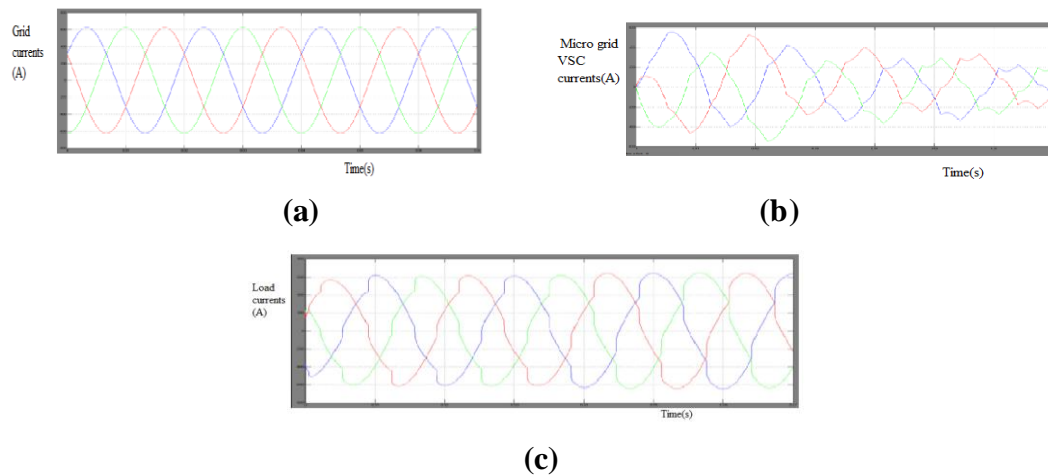


Fig.12 Simulation results using proposed control approach for micro grid side VSC (a) micro grid VSC currents (b) grid currents (c) load currents

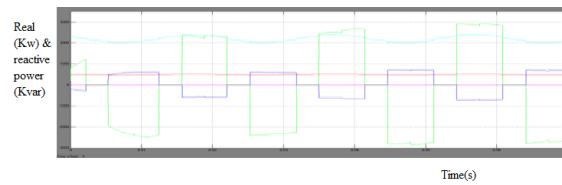


Fig.13 Real and Reactive power flow waveforms of PV hybrid generating system

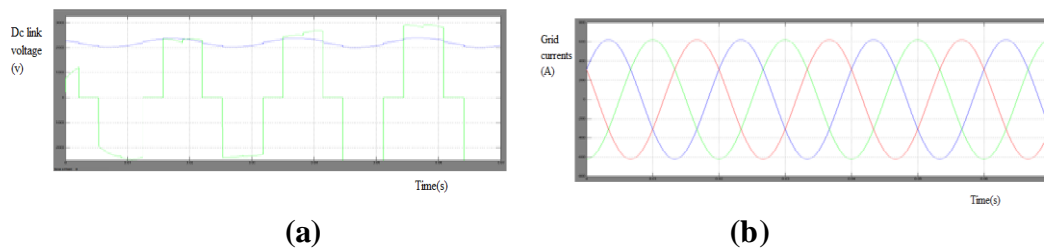


Fig.14 Simulation results performance of proposed control approach (a) dc link voltage dynamics with different in isolations(b)Grid voltages and currents

V. CONCLUSIONS

Grid integration of PV/Battery hybrid energy conversion system has been demonstrated with the application of HGICB converter topology to the PV cell is used to track the MPPT with high gain and less current ripples. The application of modified instantaneous symmetrical components theory to μ G-VSC for battery converter to regulate the dc bus voltage tightly under varying solar insolation and dc load conditions. The μ G-VSC is actively controlled to inject the generated active power to compensate the harmonic and reactive power demanded by the unbalanced and non-linear load at PCC, such that the current drawn from grid is purely sinusoidal at UPF.

REFERENCES

- [1] Energy for future I Renewable source of Energy-white paper for a community strategy and action plan, nov.26, 1997.
- [2] M.G, Villalva, J.R.Gazoli, and E.R fidho, "comprehensive approach to modeling and simulation of photovoltaic arrays", IEEE trans. power electronic vol.24, no.5, pp.1198-1208, may 2009.
- [3] v.Salas, E.olias, A, Barrado, and A.Lazaro, "review of the maximum power point tracking algorithmfor stand line.photovoltaic system ", "solar cells, vol.90, no.11, pp.1555-1578, 2006.
- [4] T.Esram and P.L.chapman, "comparision of photovoltaic array maximum power point tracking techniques" IEEE trans.energy conv, vol.22, pp.439-449.jun 2007

- [5] T.T.N.khatib, A.Mohamed, N.Amin, and K.Sopian "An efficient maximum power point tracking controller for photovoltaic systems using new boost converter design and imprived control algorithm", WSEAS trans, power system, vol.5, no.2, pp.53-63, 2010.
- [6] W. Li and X. He, "Review of non isolated high-step-up dc/dc converters in photovoltaic grid-connected applications, " IEEE Trans. Ind. Electron., vol. 58, no. 4, pp. 1239-1250, Apr. 2011.
- [7] A.Engler."control of converters in isolated and in grid tied operation with regard to expandability in tutorial: power electronics for regenerative energy", presented at the proc. IEEE power electron. spec. conf., Aachen Germany, 2004.
- [8] k.DeBrabandere, B.Bolsens, J.Vandin key bus, A.Woyte, J.driesen and R.Belmans, "A voltage frequenecy drop control method for parallel inverter", IEEEtrans.Power electron; vol.22, no.4, PP.1107-1115, jul.2007.
- [9] C.Meza, J.J.Negroni, D.Biel, and F.Guinjoan, "energy balance modeling and discrete control inverters", IEEE trans, IND, Electron, vol.55, no.7, PP.2734-2743, +.jul.2008
- [10] J.Y.Dai, D.D.X4 and B.W4, "A novel control scheme for current source converters based PMSG wind energy conversion systems", IEEE trans.power electron, vol.24, no..4, PP.963-972, Apr, 2009.
- [11] A. Chatterjee, A. Keyhani, and D. Kapoor, "Identification of photovoltaic source models, " IEEE Trans. Energy Convers., vol. 26, no. 3, pp. 883-889, Sept. 2011.
- [12] A. Rahimi, G. Williamson, and A. Emadi, "Loop-cancellation technique: A novel nonlinear feedback to overcome the destabilizing effect of constant-power loads, " IEEE Trans. Veh. Technol., vol. 59, no. 2, pp. 650-661, Feb. 2010.
- [13] A. Radwan and Y. Mohamed, "Modeling, analysis, and stabilization of converter-fed ac microgrids with high penetration of converter-interfaced loads, " IEEE Trans. Smart Grid., vol. 3, no. 3, pp. 1213-1225, Sept. 2012.
- [14] W. Tang, F. Lee, and R. Ridley, "Small-signal modeling of average current-mode control, " IEEE Trans. Power Electron., vol. 8, no. 2, pp. 112-119, Apr. 1993.
- [15] J. Carrasco, L. Franquelo, J. Bialasiewicz, E. Galvan, R. Guisado, M. Prats, J. Leon, and N. Moreno-Alfonso, "Power-electronic systems for the grid integration of renewable energy sources: A survey, " IEEE Trans. Ind. Electron., vol. 53, no. 4, pp. 1002-1016, Jun. 2006.
- [16] M. de Brito, L. Galotto, L. Sampaio, G. de Azevedo e Melo, and C. Canesin, "Evaluation of the main mppt techniques for photovoltaic applications, " IEEE Trans. Ind. Electron., vol. 60, no. 3, pp. 1156-1167, Mar. 2013.

